Mon. Not. R. astr. Soc. (1986) **221,** 553–569

On the dynamical evolution of a spheroidal cluster – II. Anisotropic velocity distribution

G. Som Sunder and R. K. Kochhar *Indian Institute of Astrophysics, Bangalore 560034, India*

Accepted 1986 February 19. Received 1986 January 10; in original form 1985 September 30

Summary. Starting from the equation of continuity in phase space we set up the macroscopic equations for collisionless stellar systems. We recover the tensor virial equation and obtain, for the first time, the tensor equivalent of the energy equation, which gives the rate of change of the kinetic energy tensor $\boldsymbol{K}_{ij}$.

These equations are then used to study the dynamical evolution of homogeneous spheroidal stellar systems where the velocity distribution is not assumed to be isotropic as has been done in previous investigations along these lines. Relaxation of the constraint of velocity isotropy significantly affects the evolution of the cluster.

When the 'pressure' is zero, the system's behaviour is identical to that of a pressureless gas cloud (Lin, Mestel & Shu).

In the general case when pressure is non-zero, and the total energy is negative, the cluster executes finite amplitude oscillations both in size and eccentricity. However, unlike in the isotropic case, the amplitude of the oscillations depends on the initial eccentricity; and the system does not oscillate between prolate and oblate shapes.

When the total energy is positive, the system expands and is eventually dispersed. However, unlike in the isotropic case, an oblate (prolate) system remains oblate (prolate). We also show that these results apply even in the case of heterogeneous spheroids.

1 Introduction

Chandrasekhar & Elbert (1972) have used the scalar virial equation to study the dynamical evolution of a spherical stellar system. Using the relation for energy conservation

$$K+W=E=\text{a constant}, \tag{1}$$

they rewrite the virial equations in the form

$$\frac{1}{2}\frac{d^2I}{dt^2}=2K+W=2E-W. \tag{2}$$

Since both I and W can be expressed in terms of the radius, a, this equation gives the radius as a function of time.

Chandrasekhar & Elbert (1972) also use the tensor virial equation

$$\frac{1}{2}\frac{d^2}{dt^2}I_{ij}=2K_{ij}+W_{ij}, \tag{3}$$

to study the dynamical evolution of a spheroidal cluster of mass points under the simplifying assumption that the velocity distribution is (always) locally isotropic so that

$$K_{11}=K_{22}=K_{33}=\tfrac{1}{3}K. \tag{4}$$

The case of negative total energy has been reexamined by Som Sunder & Kochhar (1985, Paper I), where it is shown that the system executes finite amplitude oscillations between prolate and oblate shapes.

Here we consider the general case when the artificial constraint of an isotropic velocity distribution is removed. For this we require a relation expressing the variation of the total kinetic energy tensor Ki_j with time. Such a relation, which is the tensor equivalent of the law of energy conservation (1), can be obtained from the equations of motion for an N-body system (*cf.* Som Sunder 1985). The evaluation of the quantities involved in this expression, however, require the assumption of certain symmetries in both the mass and velocity distribution. For this reason it is simpler to obtain these expressions for a system described by a continuous distribution function $f(\mathbf{x}, \mathbf{u}, t)$. This is the procedure adopted in the following section. In Section 3 we use these equations to study the collapse of 'pressureless' homogeneous stellar systems. In Section 4 the evolution of homogeneous systems with negative total energies is studied whereas Section 5 considers the case of systems with positive energies. Section 6 then studies the evolution of heterogeneous spheroids.

2 The basic equations

We consider a stellar system, a star cluster or a galaxy, consisting of a large number, N, of stars assumed to be mass points. The position, velocity, and acceleration of a particle with respect to an arbitrary frame of reference are denoted by $\mathbf{x}$, $\mathbf{u}$, $\mathbf{g}$ while $\mathbf{z}=(\mathbf{x}, \mathbf{u})$ represents the phase coordinate. Since N is large the phase space representation can be taken to be a continuous fluid with phase density given by the distribution function $f(\mathbf{z}, t)\equiv f(\mathbf{x}, \mathbf{u}, t)$ (Lynden-Bell 1969). The various tensors of interest can be defined in terms of the distribution function $f(\mathbf{z}, t)$.

The expressions for the moment of inertia, momentum, kinetic energy, and potential energy tensors of order two are

$$I_{ij}=\int_\Gamma f(\mathbf{z})\,x_i x_j\,d\mathbf{z}=\int_\Gamma \varrho(\mathbf{x})\,x_i x_j\,d\mathbf{x}, \tag{5}$$

$$L_{i;j}=\int_\Gamma f(\mathbf{z})\,u_i x_i\,d\mathbf{z}=\int_V \varrho(\mathbf{x})\,\bar{u}_i x_i\,d\mathbf{x}, \tag{6}$$

$$K_{ij}=\tfrac{1}{2}\int_\Gamma f(\mathbf{z})\,u_i u_j\,d\mathbf{z}=\tfrac{1}{2}\int_V \varrho(\mathbf{x})\,\overline{u_i u_j}\,d\mathbf{x}, \tag{7}$$

$$W_{ij}=-\frac{G}{2}\int_\Gamma\int_\Gamma f(\mathbf{z})f(\mathbf{z}')\frac{(x_i-x_i')(x_j-x_j')}{|\mathbf{x}-\mathbf{x}'|^3}\,d\mathbf{z}\,d\mathbf{z}'$$

$$=-\frac{G}{2}\int_V\int_V \varrho(\mathbf{x})\varrho(\mathbf{x}')\frac{(x_i-x_i')(x_j-x_j')}{|\mathbf{x}-\mathbf{x}'|^3}\,d\mathbf{x}\,d\mathbf{x}'. \tag{8}$$

Here Γ represents the instantaneous phase-volume of the phase fluid; V the volume of the

stellar system in coordinate-space; $\varrho(\mathbf{x})$ and $\bar{q}(\mathbf{x})$ the density and the mean value of $q(\mathbf{z})$ for all the particles at $\mathbf{x}$. The expression for $\boldsymbol{W}_{ij}$ in terms of $f(\mathbf{z})$ is a generalization of the definition of the potential energy as given by Lynden-Bell (1969). The second expressions in the right of equations (5)–(8) are obtained by effecting an integration over the entire velocity space (*cf.* Binney 1982).

The dual of the tensor $\boldsymbol{L}_{i;j}$ is the angular momentum of the system

$$\lambda_k=\sum_{ij}\varepsilon_{kji}\boldsymbol{L}_{i;j}. \tag{9}$$

(Note: the summation convention is not employed in this paper.) We write

$$u_i=\bar{u}_i+\tilde{u}_i, \tag{10}$$

where $\tilde{u}_i$ is the random velocity of the star. Then we can rewrite equation (7) in the form (*cf.* Binney 1982)

$$\boldsymbol{K}_{ij}=\boldsymbol{T}_{ij}+\tfrac{1}{2}\boldsymbol{\Pi}_{ij}, \tag{11}$$

where

$$\boldsymbol{T}_{ij}=\tfrac{1}{2}\int_V\varrho(\mathbf{x})\,\bar{u}_i\bar{u}_j\,d\mathbf{x},$$

$$\boldsymbol{\Pi}_{ij}=\int_V\varrho(\mathbf{x})\,\overline{\tilde{u}_i\tilde{u}_j}\,d\mathbf{x} \tag{12}$$

represent respectively the contributions to the kinetic energy tensor from the mean and random motions.

We define the moments of the accleration field namely the virial

$$\boldsymbol{U}_{i;j}=\int_\Gamma f(\mathbf{z})\,g_i x_j\,d\mathbf{z}=\int_V\varrho(\mathbf{x})\,\bar{g}_i x_j\,d\mathbf{x}, \tag{13}$$

and the 'H-tensor'

$$\boldsymbol{H}_{i;j}=\int_\Gamma f(\mathbf{z})\,g_i u_j\,d\mathbf{z}=\int_V\varrho(\mathbf{x})\,\overline{\tilde{g}_i\tilde{u}_j}\,d\mathbf{x}. \tag{14}$$

We assume that the system is collisionless. The distribution function then satisfies the equation of continuity (Lynden-Bell 1969)

$$\frac{\partial f}{\partial t}+\sum_{p=1}^{3}\frac{\partial}{\partial x_p}fu_p+\sum_{p=1}^{3}\frac{\partial}{\partial u_p}fg_p=0, \tag{15}$$

from which the following theorem results:

Theorem: If $q(\mathbf{z}, t)$ is an attribute of an element of the phase fluid at $\mathbf{z}$ then

$$\frac{d}{dt}\int_\Gamma f(\mathbf{z}, t)\,q(\mathbf{z}, t)\,d\mathbf{z}=\int_\Gamma f(\mathbf{z}, t)\frac{dq}{dt}d\mathbf{z}, \tag{16}$$

where

$$\frac{dq}{dt}=\frac{\partial q}{\partial t}+\sum_{p=1}^{3}u_p\frac{\partial q}{\partial x_p}+\sum_{p=1}^{3}g_p\frac{\partial q}{\partial u_p} \tag{17}$$

is the total time derivative as we follow the element in its motion through phase-space, and the integration is carried out over Γ, the instantaneous phase-volume of the phase-fluid. The proof

is analogous to that of the corresponding theorem in hydrodynamics (*cf.* Chandrasekhar 1969). By substituting various expressions for q in equation (16) we obtain the various macroscopic equations.

Thus with $q=x_i x_j$ equation (16) yields

$$\frac{dI_{ij}}{dt}=L_{i;j}+L_{j;i}. \tag{18}$$

Similarly setting $q=u_i x_j$ in equation (16) we obtain

$$\frac{d}{dt}L_{i;j}=2K_{ij}+U_{i;j}. \tag{19}$$

Combining equations (18) and (19) we get the virial equation

$$\frac{d^2I_{ij}}{dt}=4K_{ij}+(U_{i;j}+U_{j;i}). \tag{20}$$

Multiplying equation (19) by ε_{kji} and summing over i and j we obtain the equation for the rate of change of angular momentum

$$\frac{d\lambda_k}{dt}=\sum_{i,j=1}^{3}\varepsilon_{kji}U_{i;j}. \tag{21}$$

Virial equations of other orders may be obtained in an analogous fashion from equation (16) (*cf.* Som Sunder 1985).

Substituting $q=u_i u_j$ in equation (16) one obtains

$$2\frac{d}{dt}K_{ij}=H_{i;j}+H_{j;i}. \tag{22}$$

The contracted version of equation (22) expresses the variation of the total energy with time and in the case of isolated systems, reduces to the energy conservation law (1) (*cf.* Som Sunder 1985).

The relations (20)–(22) apply to any (collisionless) stellar system. We shall now confine our attention to isolated non-rotating spheroidal stellar systems. In this case

$$g_i=\frac{\partial\mathscr{V}}{\partial x_i}, \tag{23}$$

with the potential $\mathscr{V}(\mathbf{x})$ given by

$$\mathscr{V}(\mathbf{x})=G\int_\Gamma f(\mathbf{z}')\frac{1}{|\mathbf{x}-\mathbf{x}'|}d\mathbf{z}'=G\int_v \varrho(\mathbf{x})\frac{1}{|\mathbf{x}-\mathbf{x}'|}d\mathbf{x}'. \tag{24}$$

The virial therefore reduces to

$$U_{i;j}=-\frac{G}{2}\int_\Gamma\int_\Gamma f(\mathbf{z})f(\mathbf{z}')\frac{(x_i-x_i')(x_j-x_j')}{|\mathbf{x}-\mathbf{x}'|^3}d\mathbf{z}\,d\mathbf{z}'=W_{ij}, \tag{25}$$

and equation (20) takes the familiar form

$$\frac{1}{2}\frac{d^2I_{ij}}{dt^2}=2K_{ij}+W_{ij}, \tag{26}$$

whereas equation (21) reduces to the law of angular momentum conservation

$$\frac{d}{dt}\lambda_k=0. \tag{27}$$

In order to evaluate $\boldsymbol{H}_{i;j}$ we choose the coordinate axes along the body axes of the spheroid and assume that the mean velocity is a linear function of the coordinates (*cf.* Chandrasekhar 1969)

$$\bar{u}_i=\sum_{p=1}^{3}\boldsymbol{q}_{ip}x_p. \tag{28}$$

Hence making use of the fact that in the chosen frame of reference both $\boldsymbol{I}_{ij}$ and $\boldsymbol{W}_{ij}$ are diagonal we have from equations (6) and (14)

$$\boldsymbol{L}_{i;j}=\int_V \varrho(\mathbf{x})\,\bar{u}_i x_j\,d\mathbf{x}=\boldsymbol{q}_{ij}\boldsymbol{I}_{jj}, \tag{29}$$

$$\boldsymbol{H}_{i;j}=\int_V \varrho(\mathbf{x})\frac{\partial \mathscr{V}}{\partial x_i}\bar{u}_j\,d\mathbf{x}=\sum_{p=1}^{3}\boldsymbol{q}_{jp}\boldsymbol{W}_{ip}=\boldsymbol{q}_{ji}\boldsymbol{W}_{ii}. \tag{30}$$

Since by assumption the system is non-rotating

$$\lambda_k=\sum_{i,j=1}^{3}\boldsymbol{\varepsilon}_{kji}\boldsymbol{L}_{i;j}=0. \tag{31}$$

Using equations (18), (29) and (31) we have

$$\boldsymbol{q}_{ii}=\frac{1}{2\boldsymbol{I}_{ii}}\left(\frac{d\boldsymbol{I}_{ii}}{dt}\right),\qquad \boldsymbol{q}_{ij}=0\qquad (i\neq j). \tag{32}$$

Using equations (32) in equation (30) we see that the only non-trivial equations in equation (22) are

$$\frac{d\boldsymbol{K}_{ii}}{dt}=\frac{\boldsymbol{W}_{ii}}{2\boldsymbol{I}_{ii}}\frac{d\boldsymbol{I}_{ii}}{dt}. \tag{33}$$

This equation can be integrated using equation (26) to yield

$$\boldsymbol{K}_{ii}=\frac{1}{8\boldsymbol{I}_{ii}}\left(\frac{d\boldsymbol{I}_{ii}}{dt}\right)^2+\frac{\chi_i}{2\boldsymbol{I}_{ii}}, \tag{34}$$

where χ_i are constants of integration. Combining equations (34) and (26) one obtains

$$\frac{d^2\boldsymbol{I}_{ii}}{dt^2}=\frac{1}{2\boldsymbol{I}_{ii}}\left(\frac{d\boldsymbol{I}_{ii}}{dt}\right)^2+\frac{2\chi_i}{\boldsymbol{I}_{ii}}+2\boldsymbol{W}_{ii}. \tag{35}$$

By substituting from equation (28) and (32) in equation (12) we see that

$$\boldsymbol{T}_{ii}=\frac{1}{8\boldsymbol{I}_{ii}}\left(\frac{d\boldsymbol{I}_{ii}}{dt}\right)^2, \tag{36}$$

and hence from equations (34) and (11) we have

$$\boldsymbol{\Pi}_{ii}\boldsymbol{I}_{ii}=\chi_i\equiv\text{a constant}. \tag{37}$$

Just as the virial equation can be obtained by taking the moments of the hydrodynamic equations

of continuity and momentum transport (*cf.* Binney 1982) equation (37) may be obtained by integrating the transport equation for kinetic pressure (*cf.* Delcroix 1965)

$$\varrho\left(\frac{\partial}{\partial t}\overline{\tilde{u}_i\tilde{u}_j}+\sum_{p=1}^{3}\bar{u}_p\frac{\partial}{\partial x_p}\overline{\tilde{u}_i\tilde{u}_p}\right)+\sum_{p=1}^{3}\frac{\partial}{\partial x_p}\varrho\overline{\tilde{u}_i\tilde{u}_j\tilde{u}_p}+\sum_{p=1}^{3}\varrho\overline{\tilde{u}_j\tilde{u}_p}\frac{\partial\bar{u}_i}{\partial x_p}$$

$$+\sum_{p=1}^{3}\varrho\overline{\tilde{u}_j\tilde{u}_p}\frac{\partial\bar{u}_i}{\partial x_p}+\sum_{p=1}^{3}\varrho\overline{\tilde{u}_i\tilde{u}_p}\frac{\partial\bar{u}_j}{\partial x_p}=\varrho(\overline{\tilde{g}_i\tilde{u}_j}+\overline{\tilde{u}_i\tilde{g}_j}), \tag{38}$$

after introducing the approximation (28) (*cf.* Som Sunder 1985). It should be noted that equation (37) in the case of a sphere reduces to the well-known adiabatic law for a monoatomic gas.

We will be chiefly concerned with homogeneous spheroidal stellar systems with axes $a_1=a_2$ and a_3. We choose our units of length mass and time such that

$$M=1, \qquad a_1=1\,(\text{at } t=0), \qquad G=1, \tag{39}$$

so that equation (35) yields the pair of independent equations

$$\frac{d^2a_1}{dt^2}=\frac{c_1}{2a_1^3}-\frac{3}{2}\frac{1}{a_1a_3}A_1, \tag{40}$$

$$\frac{d^2a_3}{dt^2}=\frac{c_3}{2a_3^3}-\frac{3}{2}\frac{1}{a_1^2}A_3, \tag{41}$$

where

$$c_i=50\chi_i; \tag{42}$$

and the index symbols A_i for a spheroid are given by (Chandrasekhar 1969)

$$A_1=A_2=\frac{\sqrt{1-y}}{y}S(y)-\frac{1-y}{y}, \tag{43}$$

$$A_3=\frac{2}{y}-\frac{2\sqrt{1-y}}{y}S(y), \tag{44}$$

with

$$y=1-a_3^2/a_1^2, \tag{45}$$

$$S(y)=\begin{cases}\dfrac{\sin^{-1}\sqrt{y}}{\sqrt{y}} & y>0\\ 1 & y=0\\ \dfrac{\sinh^{-1}\sqrt{-y}}{\sqrt{-y}} & y<0.\end{cases} \tag{46}$$

In the following sections we use these equations to study the dynamical evolution of isolated stellar systems for various initial conditions. The constancy of the expressions for the total energy

(equation 1)

$$E=K+W=\sum_{p=1}^{3}\left[\frac{1}{8I_{pp}}\left(\frac{dI_{pp}}{dt}\right)^2+\frac{\chi_p}{2I_{pp}}\right]+W$$

$$=\frac{1}{10}\left[2\left(\frac{da_1}{dt}\right)^2+\left(\frac{da_3}{dt}\right)^2+2\frac{c_1}{2a_1^2}+\frac{c_3}{2a_3^2}\right]-\frac{3}{5}\frac{1}{a_1}S(y) \tag{47}$$

will serve as a check on the accuracy of the computation.

3 Collapse of 'pressureless' systems

In this section we investigate systems with zero 'pressure' initially, i.e.

$$\Pi_{ii}=0 \qquad \text{at } t=0. \tag{48}$$

From equation (37) it follows that the relation (48) holds for all t, i.e. the system remains pressureless, and since

$$\chi_i=c_i=0, \tag{49}$$

equations (40) and (41) take the form

$$\frac{d^2a_1}{dt^2}=-\frac{3}{2}\frac{1}{a_1a_3}A_1, \tag{50}$$

$$\frac{d^2a_3}{dt^2}=-\frac{3}{2}\frac{1}{a_1^2}A_3. \tag{51}$$

The equations are identical (except for multiplying factors) with equations (17) and (18) of Lin, Mestel & Shu (1965) who consider the evolution of a spheroidal pressureless gas cloud. Thus the behaviour of a 'pressureless' stellar system is similar to that of a pressureless gas cloud.

The results of numerical integration of equations (50) and (51) for the following initial conditions

$$\frac{da_1}{dt}=\frac{da_3}{dt}=0, \qquad y=y_0, \qquad (\text{at } t=0), \tag{52}$$

are shown in Figs 1 and 2.

In the spherical case $a_1=a_3=a$, the solution is given by the analytic expression

$$t=\frac{1}{\sqrt{2}}[\sqrt{a(1-a)}+\tfrac{1}{2}\cos^{-1}(2a-1)]. \tag{53}$$

In the spheroidal case, proceeding in a fashion similar to that of Lin *et al.* (1965), we obtain an approximate series solution

$$a_1=\cos^2\theta,$$

$$t=\frac{1}{\alpha^{(0)}}\left[(\theta+\tfrac{1}{2}\sin 2\theta)-\frac{\alpha^{(2)}}{\alpha^{(1)}}(\theta-\tfrac{1}{2}\sin 2\theta)\right],$$

$$y=1-\left\{E^{(0)}+E^{(2)}\tan^2\theta\left[1+\frac{E^{(4)}}{E^{(2)}}\tan\theta\right]\right\}^2, \tag{54}$$

Table 1. Values for the coefficients in the expansion 55.

y_0	$\alpha^{(0)}$	$\frac{\alpha^{(2)}}{\alpha^{(0)}}$	$E^{(0)}$	$E^{(2)}$	$\frac{E^{(4)}}{E^{(2)}}$
0.9	1.826	0.200	0.316	−0.851	0.050
0.5	1.556	0.063	0.707	−0.356	0.039
0.0	1.414	0.000	1.000	0.000	0.033
−0.5	1.327	−0.035	1.225	0.267	0.030
−0.9	1.276	−0.062	1.378	0.447	0.025

where the various coefficients are given by the following sequence of relations:

$$A_1^{(0)}=\frac{\sqrt{1-y_0}}{y_0}S(y_0)-\frac{1-y_0}{y_0},$$

$$E^{(0)}=\sqrt{1-y_0},$$

$$\alpha^{(0)}=\left[\frac{3}{E^{(0)}}A_1^{(0)}\right]^{1/2},$$

$$E^{(2)}=\frac{3}{[\alpha^{(0)}]^2}[3A_1^{(0)}-2],$$

$$A_1^{(2)}=-E^{(2)}\frac{\sqrt{1-y_0}}{y_0^2}\left[3-\frac{3-2y_0}{\sqrt{1-y_0}}S(y_0)\right],$$

$$\frac{\alpha^{(2)}}{\alpha^{(0)}}=\frac{3}{4E^{(0)}[\alpha^{(0)}]^2}\left[A_1^{(2)}-A_1^{(0)}\frac{E^{(2)}}{E^{(0)}}\right],$$

$$\frac{E^{(4)}}{E^{(2)}}=\{[S(y_0)]^2+S(y_0)\sqrt{1-y_0}-2\}/\{3[S(y_0)-\sqrt{1-y_0}]^2\}. \tag{55}$$

The values of these coefficients for a few values of y_0 are listed in Table 1. It is found that the series solution is in good agreement with the results of numerical integration.

It is seen from Fig. 1 that the smaller axis always collapses to a point. In the spherical case the collapse occurs in time $t^*=\Pi/2\sqrt{2}$. The collapse time increases with decreasing values of y_0, being larger for a prolate than for an oblate system.

The collapse is accompanied by an enhancement in the asphericity of the system. As pointed out by Binney (1980) both kinematic and dynamic processes are involved in the above effect. The kinematic effect is that, if during a collapse both short and long axes are shrinking at the same rate the short axis will go to zero before the long one. The dynamical effect, which Binney calls 'self-tidal distortion' is due to the fact that the shortest axis is subject to the greatest acceleration towards the centre, and hence collapses faster towards the centre. As a result an oblate spheroid becomes more oblate as it collapses and tends towards a disc, whereas a prolate spheroid tends towards a spindle shape.

4 Systems with negative energy and non-zero pressure

If the initial 'pressure' is even slightly non-zero, we see from equation (37) that the pressure tensor increases as the system collapses, and this in turn will stop the collapse. We now study such systems which are characterized by a total negative energy E and in initial eccentricity y_0. We further assume that initially there are no mass motions so that the entire kinetic energy is in the

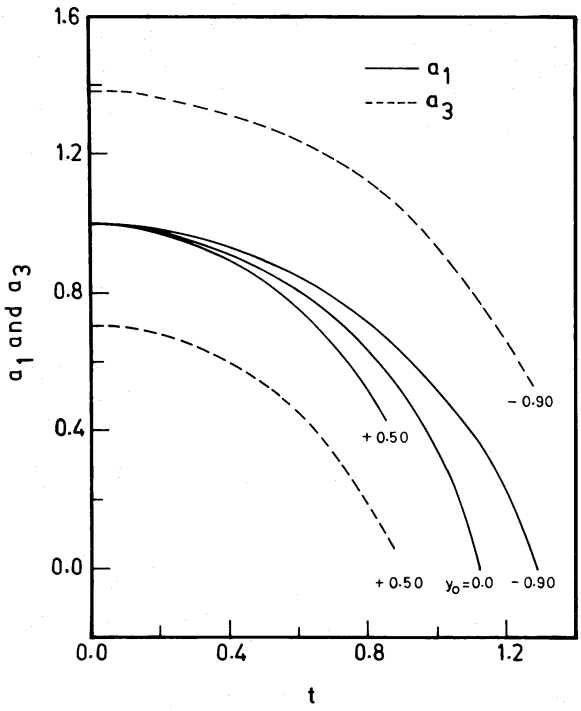

Figure 1. The evolution of homogeneous spheroidal clusters with zero 'pressure'. The figure depicts the behaviour of the two semi-axes a_1 and a_3 with respect to time measured in the units given by equation (39). The curves are labelled by the values of y_0 to which they belong.

form of random motions, which we assume are isotropic, so that at $t=0$

$$T_{11}=T_{22}=T_{33}=0, \qquad \Pi_{11}=\Pi_{22}=\Pi_{33}. \tag{56}$$

Note that the assumption of velocity isotropy is only made initially and not throughout the evolution as in Paper I. From equations (56), (36) and (47) it follows that

$$\frac{da_1}{dt}=\frac{da_3}{dt}=0 \qquad \text{at } t=0, \tag{57}$$

and that

$$c_1=4[Q+S(y_0)],$$

$$c_3=(1-y_0)\,c_1, \tag{58}$$

where

$$Q=E/|W_0|, \qquad W_0=-\tfrac{3}{5}. \tag{59}$$

W_0 is the potential energy of a sphere of unit radius. Using equation (58) we can integrate equations (40) and (41) for various values of E and y_0.

Consider first the case of a spherical stellar system, $a_1=a_3=a$. Equations (40) and (41) reduce to the single equation

$$\frac{d^2a}{dt^2}=\frac{c}{2a^3}-\frac{1}{a^2}, \tag{60}$$

with

$$c=4[Q+1]. \tag{61}$$

Equation (60) should be compared with equation 140 of Field (1975) for a collapsing gas cloud with internal pressure. It is seen that the equations are identical if $\gamma=5/3$ in Field (1975), showing that the behaviour of a spherical stellar system is identical with that of a spherical gas cloud of monoatomic particles. Equation (47) provides an integral of equation (60)

$$\frac{1}{2}\left(\frac{da}{dt}\right)^2+\frac{c}{4}\left(\frac{1}{a^2}-1\right)-\left(\frac{1}{a}-1\right)=0,$$

which in turn can be integrated to yield

$$t=\pm\sqrt{2}\left\{\frac{1}{4-c}\sqrt{(c-4)a^2+4a-c}+\frac{2}{(4-c)^{3/2}}\left[\cos^{-1}\left(\frac{(4-c)a-2}{|2-c|}\right)-\alpha\pi\right]\right\} \tag{63}$$

with $a=0$ when $c<2$, $\alpha=1$ when $c>2$.

We see from equation (63) that the system oscillates with a period

$$P=4\sqrt{2}\pi/(4-c)^{3/2}=\pi/[\sqrt{2}(-Q)^{3/2}]. \tag{64}$$

This result should be contrasted with the case of gas clouds, for which $\gamma<4/3$, and the gravitational force always dominates over the pressure term and hence the collapse is never halted (Hoyle 1953; Field 1975).

Turning now to spheroidal systems we note that the equations (40) and (41) are not the same as

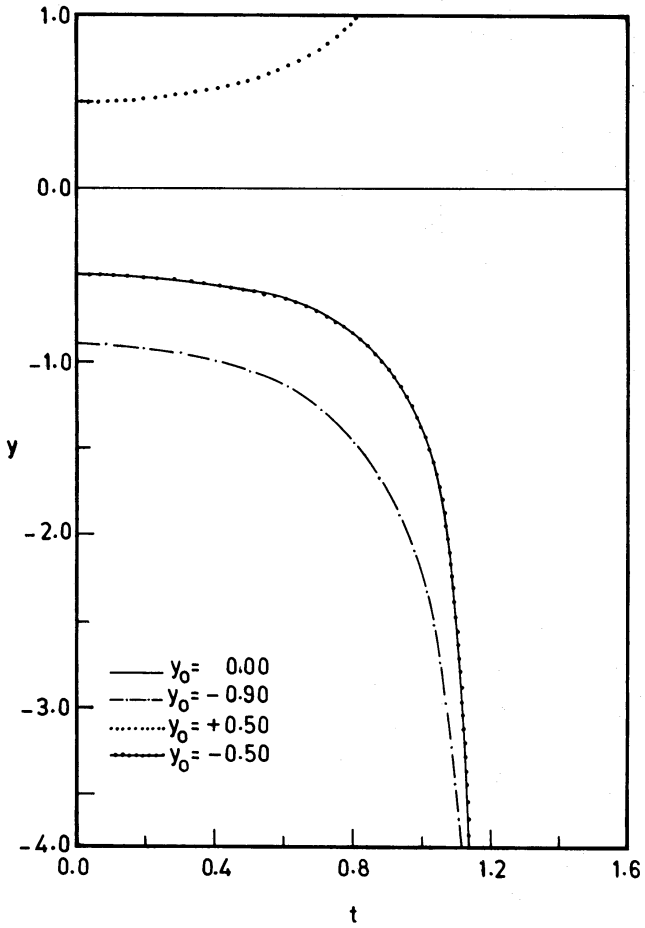

Figure 2. The evolution of homogeneous spheroidal clusters with zero 'pressure'. The ordinate y is a measure of the eccentricity (e^2), positive for oblate spheroids and negative for prolate ones. The abscissa measures time in the units given by equation (39). The curves are labelled by the values of y_0 to which they belong.

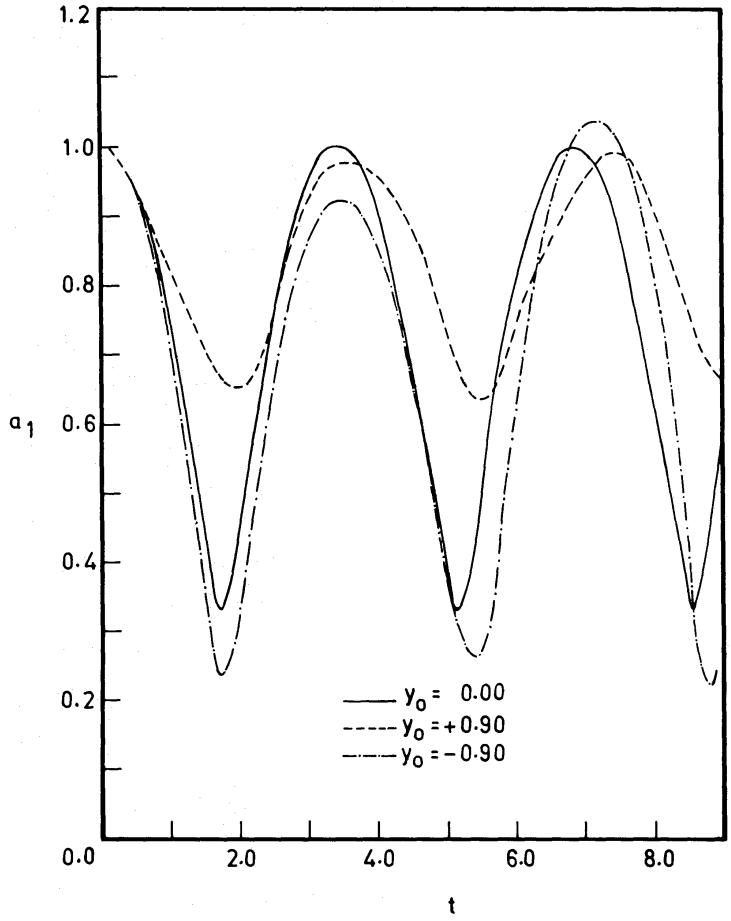

Figure 3. The evolution of homogeneous spheroidal clusters with negative total energies. Case $Q=-0.75$. The curves depict the behaviour of the semi-axis a_1 with time in the same units as Fig. 1.

those for a gas cloud (equations 133 and 134 of Field 1975). The reason is that whereas even spheroidal gas clouds are characterized by isotropic pressure, spheroidal collisionless stellar systems are not.

The results of numerical integration of equations (40) and (41) for various values of Q and y_0 are shown in Figs 3–8.

Consider first the case of $Q=-0.75$. For all y_0 considered, $K_{11}<|W_{11}|$ initially and hence the a_1 axis contracts (Fig. 3). This contraction is accompanied by an increase in pressure, which causes the system to expand once again; these oscillations have a period of about $P\simeq 3.5$ [in the units of equation (39)] which is about the same as that given by the relation (64). The amplitude of the oscillation increases with decreasing y_0. The eccentricity y also decreases initially (Fig. 4). At about $\frac{1}{2}P$, however, there is a steep rise and a fall after which the system slowly returns to $y\approx y_0$. The system does not, however, in general return to the exact initial conditions after a cycle, the only exception being when the system is spherical, in which case the behaviour is identical with that given by equation (63).

In the case when $Q=-0.25$ (Figs 5 and 6) $K_{11}>|W_{11}|$ initially for all y_0 considered and the a_1 axis expands and contracts in a period $P\approx 18$. In this case the amplitude increases with increasing y_0. The eccentricity, y, once again shows a double-wave behaviour over the same period.

The case $Q=-0.50$ (Figs 7 and 8) corresponds to equilibrium when $y_0=0$. When $y_0\neq 0$, however, the a_1 axis oscillates with a period $P\approx 6.5$ while the eccentricity shows a double-wave behaviour over approximately the same period.

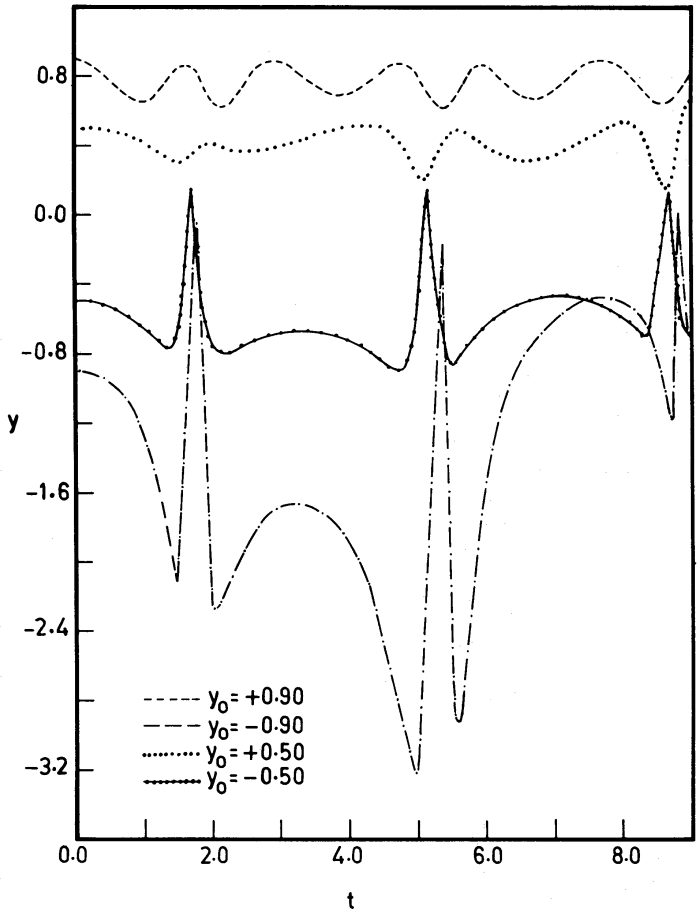

Figure 4. The evolution of homogeneous spheroidal clusters with negative total energies. Case $Q = -0.75$. The curves depict the behaviour of the eccentricity y with time in the same units as Fig. 2.

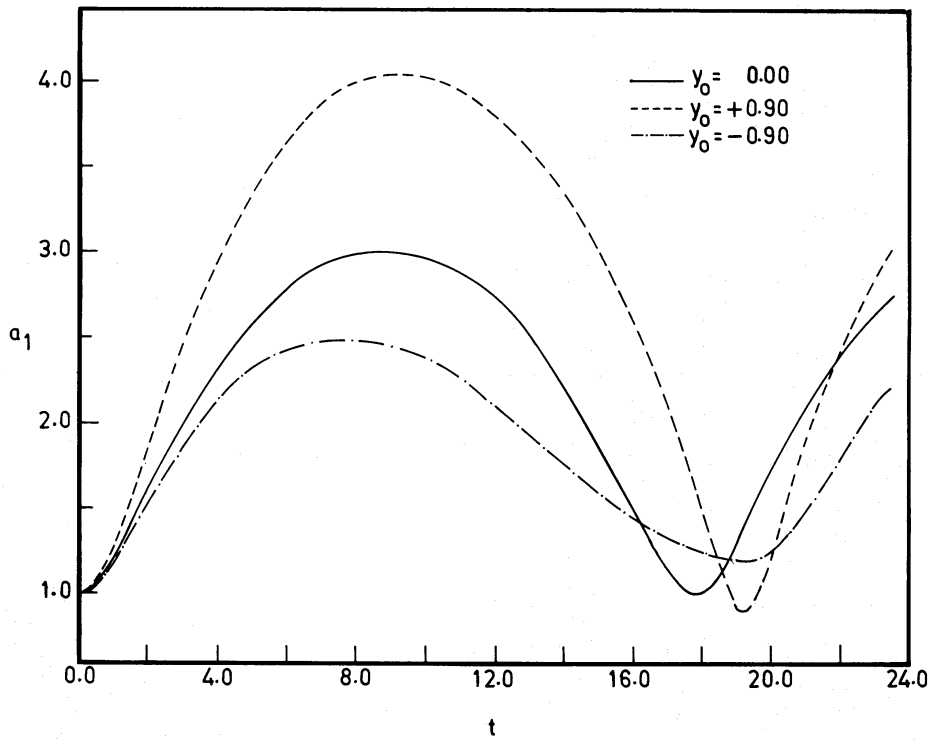

Figure 5. The evolution of homogeneous spheroidal clusters with negative total energy. Case $Q = -0.25$. The curves depict the behaviour of the semi-axis a_1 with time in the same units as Fig. 1.

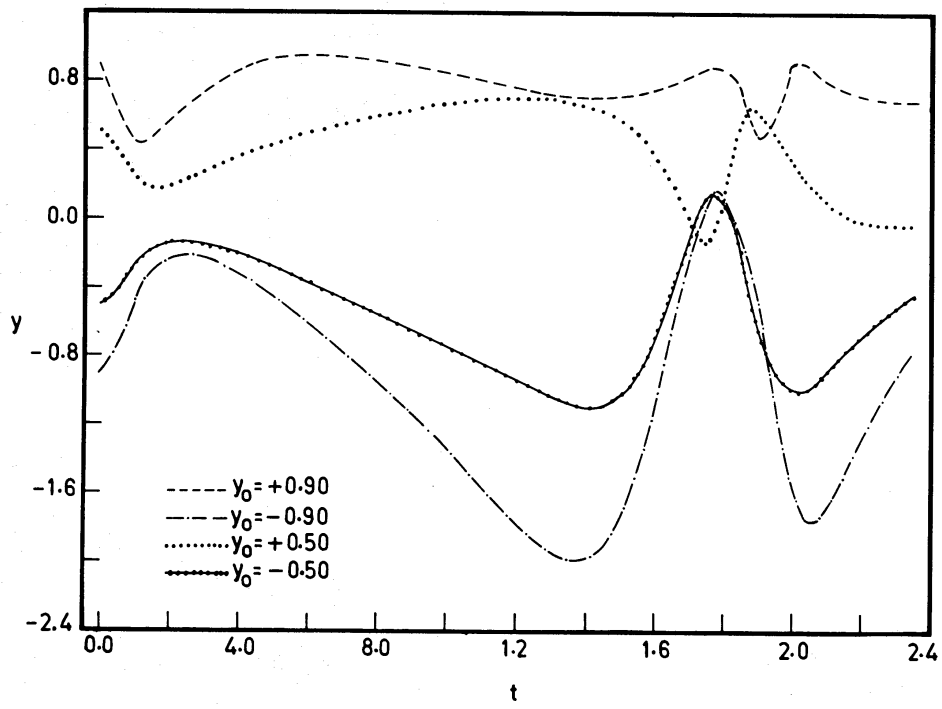

Figure 6. The evolution of homogeneous spheroidal clusters with negative total energy. Case $Q=-0.25$. The curves depict the behaviour of the eccentricity y with time in the same units as Fig. 2.

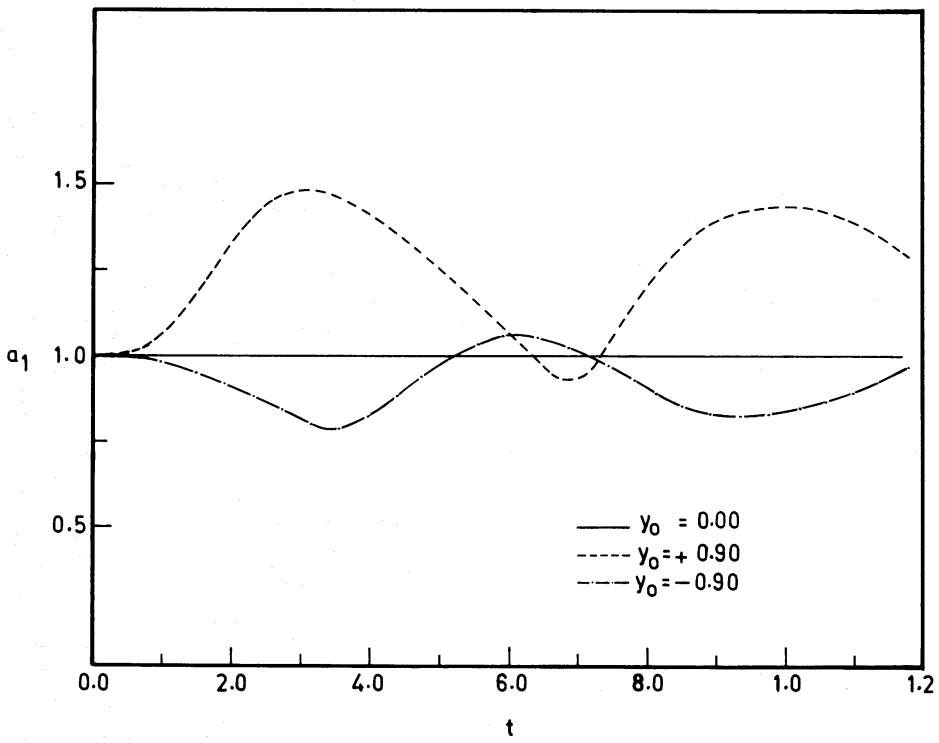

Figure 7. The evolution of homogeneous spheroidal clusters with negative total energy. Case $Q=-0.50$. The curves depict the behaviour of the semi-axis a_1 with time in the same units as Fig. 1.

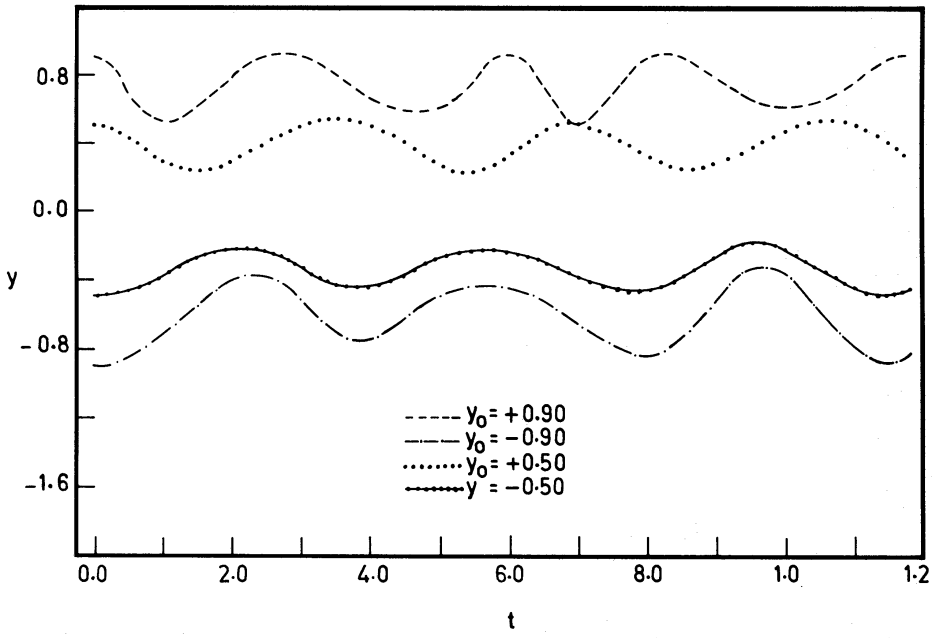

Figure 8. The evolution of homogeneous spheroidal clusters with negative total energy. Case $Q=-0.50$. The curves depict the behaviour of the eccentricity y with time in the same units as Fig. 1.

In general when the total energy is negative, i.e. $Q<0$, the a_1 axis executes finite amplitude oscillations of period $P\approx\pi/[\sqrt{2}(-Q)^{3/2}]$. The eccentricity also shows a double-wave behaviour over this period. These results should be compared with those of Paper I, where it is assumed that the velocity distribution always remains isotropic. In the anisotropic case the amplitude of the oscillations in a_1 depends upon y_0, whereas in the isotropic case it is independent of y_0. Also, though y oscillates, the system does not go from oblate to prolate or from prolate to oblate as in the isotropic velocity case.

5 Systems with positive total energy

We now consider systems with a positive total energy E and a given initial eccentricity y_0. Equations (40) and (41) have been integrated using equation (58) for $Q=E/|W_0|=0.0$, 0.5 and 1.0 and the results are illustrated in Figs 9 and 10.

It is seen from Fig. 9 that systems with positive energies expand and are eventually dispersed, systems with larger energies expanding faster. When $y_0=0$, the behaviour is given by the analytical solutions (*cf.* Chandrasekhar & Elbert 1972)

$$t=\frac{\sqrt{2}}{3}\sqrt{a-1}(a-2) \qquad \text{(when } c_1=4 \text{ or } Q=0.0\text{)}.$$

$$t=\pm\sqrt{2}\left\{\frac{1}{c-4}\sqrt{(c-4)a^2+4a-c}+\frac{2}{(c-4)^{3/2}}\cosh^{-1}\left[\frac{(c-4)a+2}{c-2}\right]\right\}$$

$$\text{(when } c_1>4 \text{ or } Q>0\text{)}. \qquad (65)$$

For the same value of Q, the more oblate the system (i.e. the greater the y_0) the faster it expands. The expansion is initially accompanied by a rapid drop in the eccentricity (Fig. 10), i.e. both oblate and prolate systems become more spherical. The eccentricity then tends to a finite limit. The results are in general agreement with those of Chandrasekhar & Elbert (1972).

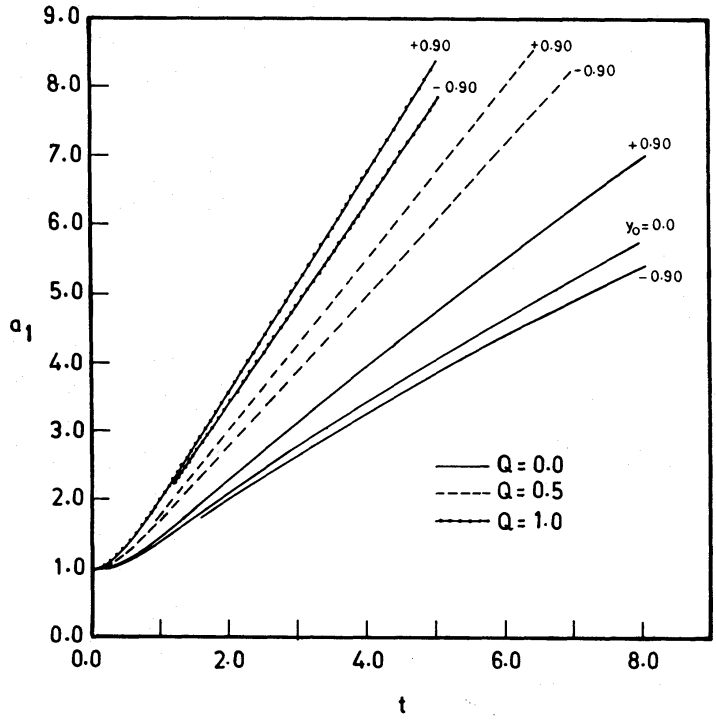

Figure 9. The evolution of homogeneous spheroidal clusters with positive total energy. The curves depict the behaviour of the semi-axis a_1 with time the same units as Fig. 1. The curves are labelled by the values of Q and y_0 to which they belong.

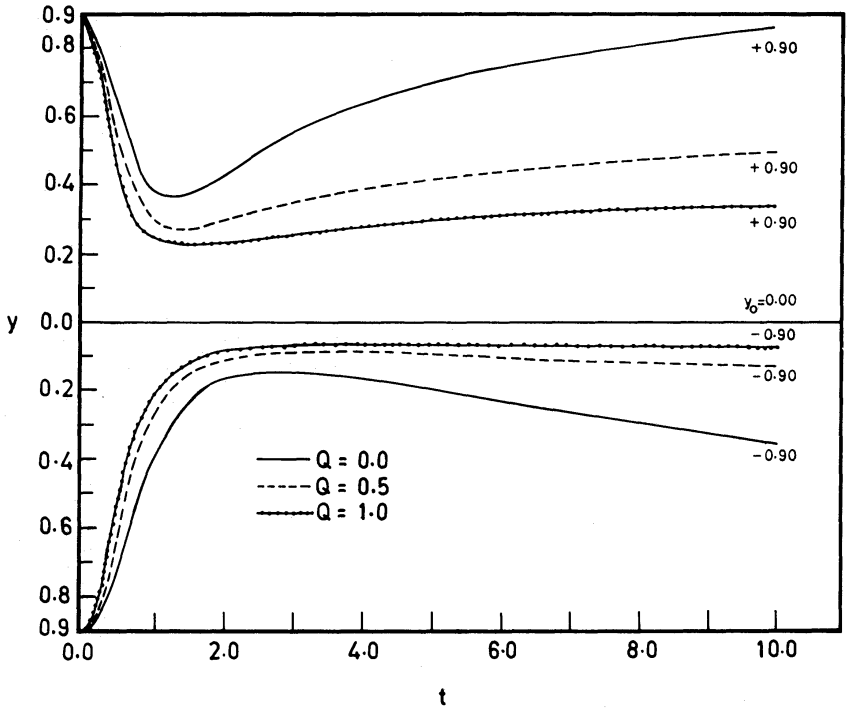

Figure 10. The evolution of homogeneous spheroidal clusters with positive total energy. The curves depict the behaviour of the eccentricity with time in the same units as Fig. 1. The curves are labelled by the values of Q and y_0 to which they belong.

However, in the present anisotropic velocity case an oblate (prolate) system remains oblate (prolate) unlike in the isotropic velocity case where the eccentricity, y, may change sign.

6 Heterogeneous spheroids

We now consider heterogeneous spheroids with density distribution of the form (*cf.* Paper I)

$$\varrho(\mathbf{x})=\varrho_c\left[1-\sum_{p=1}^{3}\frac{x_p^2}{a_p^2}\right]^{\nu} \tag{66}$$

where $\nu\geqslant 0$. The case when $\nu=0$ is that of homogeneous spheroids considered in the earlier sections. We assume that the form of the mass distribution (66) continues to be maintained as the system evolves, i.e. ν is independent of time. The moment of inertia and potential energy tensors for such a system are given in Paper I. Choosing our units of mass length and time such that

$$M=1,\ a_1=1 \qquad (\text{at } t=0), \qquad G\frac{\psi(\nu)}{\phi(\nu)}=1, \tag{67}$$

[where the functions $\phi(\nu)$ and $\psi(\nu)$ are defined and tabulated in Paper I] we obtain

$$I_{11}=\tfrac{1}{5}a_1^2\phi(\nu), \qquad I_{33}=\tfrac{1}{5}a_3^2\phi(\nu),$$

$$W_{11}=-\frac{3}{10}\frac{1}{a_1}A_1\phi(\nu), \qquad W_{33}=-\frac{3}{10}\frac{a_3}{a_1^2}A_3\phi(\nu), \tag{68}$$

and since ν is independent of time, substitution of these expressions in (35) yields the pair of expressions

$$\frac{d^2a_1}{dt^2}=\frac{c_1}{2a_1^3}-\frac{3}{2}\frac{1}{a_1a_3}A_1, \tag{69}$$

$$\frac{d^2a_3}{dt^2}=\frac{c_3}{2a_3^3}-\frac{3}{2}\frac{1}{a_1^2}A_3, \tag{70}$$

where

$$c_i=\frac{50\chi_i}{[\phi(\nu)]^2}. \tag{71}$$

Equations (69) and (70) are identical with equations (40) and (41) for a homogeneous spheroid and hence the results of the earlier sections also apply to heterogeneous spheroids.

Acknowledgment

We thank Professor Saleh Mohammed Alladin for useful discussion.

References

Binney, J., 1980. *Phil. Trans. R. Soc. London Ser. A,* **296,** 329.
Binney, J., 1982. *Morphology and Dynamics of Galaxies,* Saas-Fee, Switzerland.
Chandrasekhar, S., 1969. *Ellipsoidal Figures of Equilibrium,* Yale University Press, New Haven.
Chandrasekhar, S. & Elbert, D. D., 1972. *Mon. Not. R. astr. Soc.,* **155,** 435.
Delcroix, J. L., 1965. *Plasma Physics,* John Wiley, Chichester.

Field, G. B., 1975. *Galaxies and the Universe,* p. 359, eds Sandage, A., Sandage, M. & Kristian, J., University of Chicago Press, Chicago.

Hoyle, F., 1953. *Astrophys. J.,* **118,** 513.

Lin, C. C., Mestel, L. & Shu, F. H., 1965. *Astrophys. J.,* **142,** 1431.

Lynden-Bell, D., 1969. *Astrophysics and General Relativity,* p. 1, eds Chretien, M., Deser, S. & Goldstein, J., Gordon and Breach Science Publishers, New York.

Som Sunder, G., 1985. *PhD thesis*, Osmania University, Hyderabad.

Som Sunder, G. & Kochhar, R. K., 1985. *Mon. Not. R. astr. Soc.,* **213,** 381.